Steric Effects on the pK_a of N-Protonated *N*-Acetyl-*p*-benzoquinone Imines: Evidence for Hydration via N-Protonation

Michael Novak* and Kristy Ann Martin

Department of Chemistry, Miami University, Oxford, Ohio 45056

Received August 7, 1990

The specific acid catalyzed hydration rate constant for *N*-acetyl-*p*-benzoquinone imine (**1a**) is (7.7×10^3)-fold larger than that of its 2,6-dimethyl analogue **1b**. Since the uncatalyzed attack of small nucleophiles on C-1 of **1b** is not significantly hindered, it had been proposed that pK_a^N (eq 1) for **1a** must be ca. 3.2 units larger than that for **1b**. Little evidence was available to distinguish between the hydration mechanisms of eqs 1 and 2. Measurements of pK_a^N for the deacylated iminium ions **5a** and **5b** and the results of ab initio calculations on the structures and energies of **1–5** indicate that N-protonation of **1a** is favored over **1b** by up to 5 orders of magnitude. A combination of steric hindrance to solvation of the acidic proton in **2b** and sterically enforced destabilization of **2b** appear to be the causes of this large ΔpK_a^N. These same calculations indicate that O-protontion of **1b** is favored over that of **1a**. This result provides support for the hydration mechanism of eq 1 since the O-protonation mechanism of eq 2 would predict more rapid hydration of **1b**.

In an earlier study of the hydrolysis reactions of *N*-acetyl-*p*-benzoquinone imine (**1a**), a suspected toxic metabolite of acetaminophen,[1] and its 2,6-dimethyl analogue **1b**, we observed that the rate constant for specific acid catalyzed hydration, k_H, (k_2/K_a^N in eq 1) was (7.7×10^3)-fold larger for **1a** than for **1b**.[2] Since the rate constants for uncatalyzed attack of OH^- and H_2O on C-1 of **1a** are less than 5-fold larger than those for **1b**, it appeared that pK_a^N for **1a** must be ca. 3.2 units more positive than that for **1b**.[2] Unfortunately, direct measurement of pK_a^N is not possible due to the rapid hydration reaction.

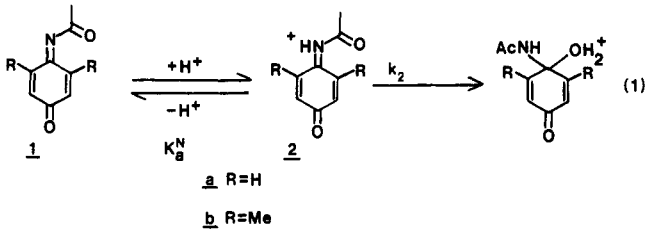

(1)

This pK_a difference was attributed to steric inhibition of solvation of **2b** by H-bonding of solvent water to the N–H. Similar effects have been observed in such species as the 2,6-di-*tert*-butylpyridinium ion.[3] Gas-phase basicity measurements appear to confirm that steric inhibition of solvation is responsible for the pK_a effects in the pyridinium ions.[4] An alternative hydration mechanism involving O-protonation (eq 2) was considered less likely because the acyl oxygen of **3b** is considerably more remote from the methyl groups than the nitrogen of **2b** according to MNDO calculations.[2] No other evidence that could distinguish between the two mechanisms was available.

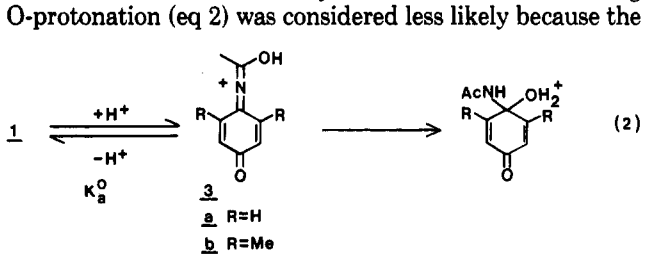

(2)

In this paper we report results of measurements of pK_a^N for the conjugate acids **5a** and **5b** of the quinone imines **4a** and **4b** (eq 3) and the results of ab initio calculations on the structures and energies of the species **1–5**. These data provide further evidence for the mechanism of eq 1 and also show that the pK_a^N differences in **2a** and **2b** are due to a combination of steric inhibition of solvation and sterically enforced conformational differences in the structures of **2a** and **2b**, which lead to destabilization of **2b**.

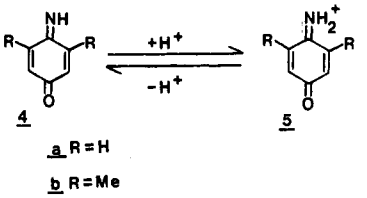

(3)

Experimental Section

Synthesis. All solvents and other materials were reagent grade and were used without further purification unless otherwise indicated. The purification of reagent grade CH_3CN has been described.[5]

***p*-Benzoquinone Imine (4a).** The imine was synthesized by oxidation of 4-aminophenol (0.01 M) in CH_3CN by excess Ag_2O at room temperature according to a published procedure.[6] Suspended solids were removed after 0.5 h by centrifugation. The CH_3CN solution of **4a** was stored at −25 °C. It decomposed over a period of 2–3 days so new solutions were prepared regularly for the kinetic measurements. Hydrolysis of the imine in 0.05 M HCl produced only *p*-benzoquinone, which was detected by HPLC comparison to an authentic sample. HPLC conditions were C-18 μ-Bondapak column, 1/1 MeOH/H_2O, 1 mL/min. UV detection was performed at 250 nm.

3,5-Dimethyl-*p*-benzoquinone Imine (4b). The imine was prepared by lead tetraacetate oxidation[7] of 4-amino-3,5-dimethylphenol, which was in turn synthesized in two steps from 3,5-dimethylphenol by nitration in dilute nitric acid, followed by reduction with basic $Na_2S_2O_4$.[8]

(1) Dahlin, D. C.; Miwa, G. T.; Lu, A. Y. H.; Nelson, S. D. *Proc. Natl. Acad. Sci. U.S.A.* **1984**, *81*, 1327–1331. Corcoran, G. B.; Mitchell, J. R.; Vaishnav, Y. N.; Horning, E. C. *Molec. Pharmacol.* **1980**, *18*, 536–542. Mulder, G. J.; Hinson, J. A.; Gillette, J. R. *Biochem. Pharmacol.* **1978**, *27*, 1641–1647. Potter, D. W.; Hinson, J. A. *J. Biol. Chem.* **1987**, *262*, 966–973.

(2) Novak, M.; Bonham, G. A.; Mulero, J. J.; Pelecanou, M.; Zemis, J. N.; Buccigross, J. M.; Wilson, T. C. *J. Am. Chem. Soc.* **1989**, *111*, 4447–4456.

(3) (a) Condon, F. E. *J. Am. Chem. Soc.* **1965**, *87*, 4494–4496. (b) Brown, H. C.; Kanner, B. *J. Am. Chem. Soc.* **1966**, *88*, 986–992.

(4) Arnett, E. M. In *Proton Transfer Reactions*; Caldin, E.; Gold, V., Eds.; Chapman and Hall: London, 1975; pp 79–101. See also: Bernasconi, C. F.; Carre, D. J. *J. Am. Chem. Soc.* **1979**, *101*, 2707–2709.

(5) Novak, M.; Pelecanou, M.; Roy, A. K.; Andronico, A. F.; Plourde, F. M.; Olefirowicz, T. M.; Curtin, T. J. *J. Am. Chem. Soc.* **1984**, *106*, 5623–5631.

(6) Willstätter, R.; Pfannenstiel, A. *Chem. Ber.* **1904**, *37*, 4605–4609.

(7) Feng, P. C. C.; Wratten, S. J. *J. Agric. Food Chem.* **1987**, *35*, 491–496.

(8) Adams, R.; Stewart, H. W. *J. Am. Chem. Soc.* **1941**, *63*, 2859–2864. Albert, H. E. *J. Am. Chem. Soc.* **1954**, *76*, 4985–4988.

0022-3263/91/1956-1585$02.50/0

The aminophenol (32.0 mg, 0.23 mmole) was dissolved in 10 mL of dried ethyl acetate stirred under a N_2 atmosphere in a 25-mL three-necked flask. Lead tetraacetate (0.25 g, 0.56 mmol) was added in one portion and the reaction mixture was stirred for 10 min. The mixture was then filtered directly into a separatory funnel and extracted twice with cold 5% aqueous $NaHCO_3$. After drying over Na_2SO_4, the ethyl acetate was removed by rotary evaporation to yield a yellowish solid, which was sublimed under reduced pressure and then recrystallized from hexanes to yield yellow needles: mp 81–83 °C; NMR (90 MHz, $(CD_3)_2CO$) δ 2.20 (3 H, s), 2.22 (3 H, s), 2.92 (1 H, s), 6.33 (1 H, s), 6.39 (1 H, s); high resolution MS, m/e 135.0696, C_8H_9NO requires 135.0685.

Kinetic Measurements. The decomposition of **4a** and **4b** was monitored in the pH range of 1.0–6.0 by UV methods with a Varian Cary 2290 spectrophotometer or an Atago Bussan RA-401 stopped flow spectrophotometer equipped with an RA-451 data processor. Hydrolysis reactions were performed in acetate and formate buffers and HCl solutions maintained at 0.1 M ionic strength with KCl. All H_2O used in the kinetic studies was distilled, deionized (18.0 MΩ cm), and distilled again in an all-glass apparatus. Dilutions of the buffer solutions were obtained by appropriate mixtures of a master buffer (0.1 M) and a 0.1 M KCl solution. Initial concentrations of the imine of ca. 5.0×10^{-5} M were obtained by 15-μL injections of a 0.01 M stock solution in CH_3CN into 3.0 mL of the aqueous buffer, or by mixing a 0.1 M KCl solution containing 1×10^{-4} M **4** with an appropriate HCl solution in the stopped flow spectrophotometer. All kinetics were performed at 20.0 ± 0.1 °C. Absorbance changes were monitored at 262 nm for **4a** and 275 nm for **4b**. Absorbance vs time data fit the first-order rate equation well for at least 4 half-lives. All pH measurements were made after the kinetic run on an Orion Model 701 A pH meter equipped with a Radiometr GK 2402C combination electrode.

Buffer-independent rate constants were obtained at each pH of the formate and acetate buffers by a linear least-squares fit of the pseudo-first-order rate constants, k_{obs}, vs total buffer concentration. In all cases four measurements were made at 0.025, 0.050, 0.075, and 0.100 M in total buffer. Initial absorbances of **4b** at 275 nm were also fit by a least-squares method to a standard titration curve for a weak acid. Further treatment of the data is described in the Results section.

Product Analyses. Product studies were performed by HPLC on a μ-Bondapak C-18 column: 1/1 MeOH/H_2O, 1 mL/min. UV measurements were made at 250 and 225 nm. Random acetate, formate, and HCl runs were analyzed by triplicate injections of the final reaction mixture (10 μL). Comparisons were made to authentic samples of *p*-benzoquinone and 2,6-dimethyl-*p*-benzoquinone.[2]

Calculations. Restricted Hartree–Fock calculations were performed with the GAUSSIAN86 and GAUSSIAN88 programs.[9] GAUSSIAN86 was installed on the IBM 4381/23 at Miami. GAUSSIAN88 was utilized on the Cray Y-MP8/864 at the Ohio Supercomputer Center. Complete geometry optimizations were performed on structures **1-5a** and **1-5b** with both the minimal STO-3G[10] and split-valence 3-21G[11] basis sets and the default BERNY optimization routine[12] of the GAUSSIAN programs. Initial force constants for the optimizations were calculated from the AM1[13] model by use of the MNDOFC option. Rotational potentials about the C(O)–N bond of **1a** and **2a** were examined by geometry optimizations (STO-3G) at fixed rotation angles at 20° intervals. Single point calculations employing the polarization basis set 6-31G*[14] and the second-order Moller–Plesset correlation energy correction[15] were performed on the optimized 3-21G structures in several cases.

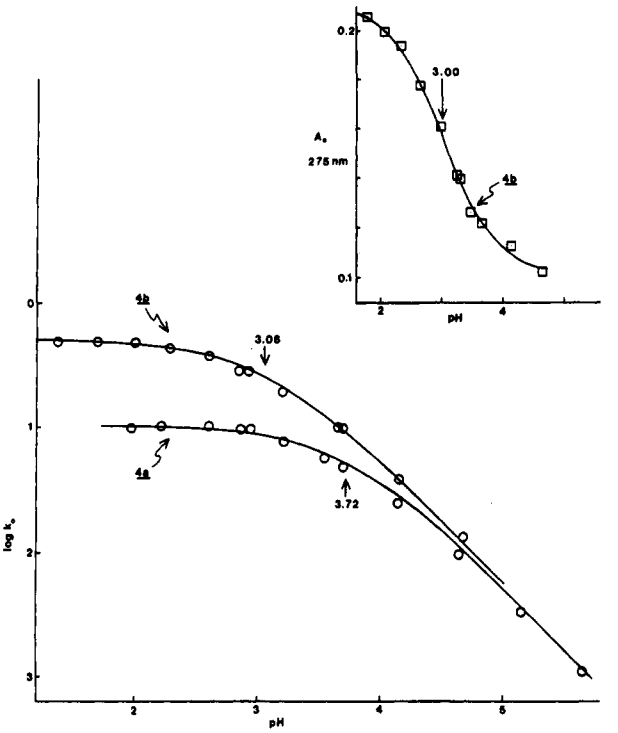

Figure 1. Log k_0 vs pH for the hydrolysis of **4a** and **4b** at 20 °C. Data were fit to eq 5 by nonlinear least-squares methods. The derived pK_a^Ns are indicated. Insert: Initial absorbance at 275 nm vs pH for **4b**. The data were fit to a standard titration curve for a weak acid. The derived pK_a^N is indicated.

Table II. Kinetic Parameters of Equation 5 for 4a and 4b[a]

	k_s, s^{-1}	K_a^N, M^{-1}	pK_a^N
4a	$1.03 \pm 0.02 \times 10^{-1}$	$1.91 \pm 0.30 \times 10^{-4}$	3.72 ± 0.06
4b	$5.13 \pm 0.09 \times 10^{-1}$	$8.67 \pm 0.45 \times 10^{-4}$	3.06 ± 0.03

[a] Conditions μ = 0.10 M (KCl), T = 20 °C, no attempt was made to extrapolate the measured pK_a^N to zero ionic strength.

Results

The hydrolysis reactions of both **4a** and **4b** were cleanly first-order under all conditions examined (pH ca. 1.0 – 6.0, μ = 0.10 M, T = 20 °C). In formate and acetate solutions weak buffer catalysis was observed and the rate data were fit well by eq 4. Values of k_0 obtained from least-squares

$$k_{obs} = k_0 + k_B[B_T] \quad (4)$$

treatment of k_{obs} vs $[B_T]$ in the buffers and k_0 obtained in HCl solutions are presented in Table I in the supplementary material. The only hydrolysis products observed by HPLC analysis of reaction mixtures were *p*-benzoquinone for **4a** and 2,6-dimethyl-*p*-benzoquinone for **4b**. The average yield of *p*-benzoquinone obtained from five randomly chosen kinetic runs of **4a** was 86.4 ± 1.4%, while the average yield of 2,6-dimethyl-*p*-benzoquinone obtained from seven randomly chosen kinetic runs of **4b** was 94.7 ± 6.8%. The yields of *p*-benzoquinone are based on an assumed stock solution concentration since the CH_3CN stock solution of **4a** was prepared without isolation of **4a**

(9) GAUSSIAN86: Frisch, M. J.; Binkley, J. S.; Schlegel, H. B.; Raghavachari, K.; Melius, C. F.; Martin, R. L.; Stewart, J. J. P.; Bobrowicz, F. W.; Rohlfing, C. M.; Kahn, L. R.; Defrees, D. J.; Seger, R.; Whiteside, R. A.; Fox, D. J.; Fleuder, E. M.; Pople, J. A. Carnegie-Mellon Quantum Chemistry Publishing Unit, Pittsburgh, PA, 1984. GAUSSIAN88: Frisch, M. J.; Head-Gordon, M.; Schlegel, H. B.; Raghavachari, K.; Binkley, J. S.; Gonzalez, C.; Defrees, D. J.; Fox, D. J.; Whiteside, R. A.; Seeger, R.; Melius, C. F.; Baker, J.; Martin R.; Kahn, L. R.; Stewart, J. J. P.; Fluder, E. M.; Topiol, S.; Pople, J. A. Gaussian, Inc., Pittsburg, PA, 1988.

(10) Hehre, W. J.; Stewart, R. F.; Pople, J. A. *J. Chem. Phys.* **1969**, *51*, 2657–2664.

(11) Binkley, J. S.; Pople, J. A.; Hehre, W. J. *J. Am. Chem. Soc.* **1980**, *102*, 939–947. Gordon, M. S.; Binkley, J. S.; Pople, J. A.; Pietro, W. J.; Hehre, W. J. *J. Am. Chem. Soc.* **1982**, *104*, 2797–2803.

(12) Schlegel, H. B. *J. Comp. Chem.* **1982**, *3*, 214–218.

(13) Dewar, M. J. S.; Zoebisch, E. G.; Healy, E. F.; Stewart, J. P. *J. Am. Chem. Soc.* **1985**, *107*, 3902–3909.

(14) Hariharan, P. C.; Pople, J. A. *Theoret. Chim. Acta* **1973**, *28*, 213–222.

(15) Moller, C.; Plesset, J. S. *Phys. Rev.* **1934**, *46*, 618–622.

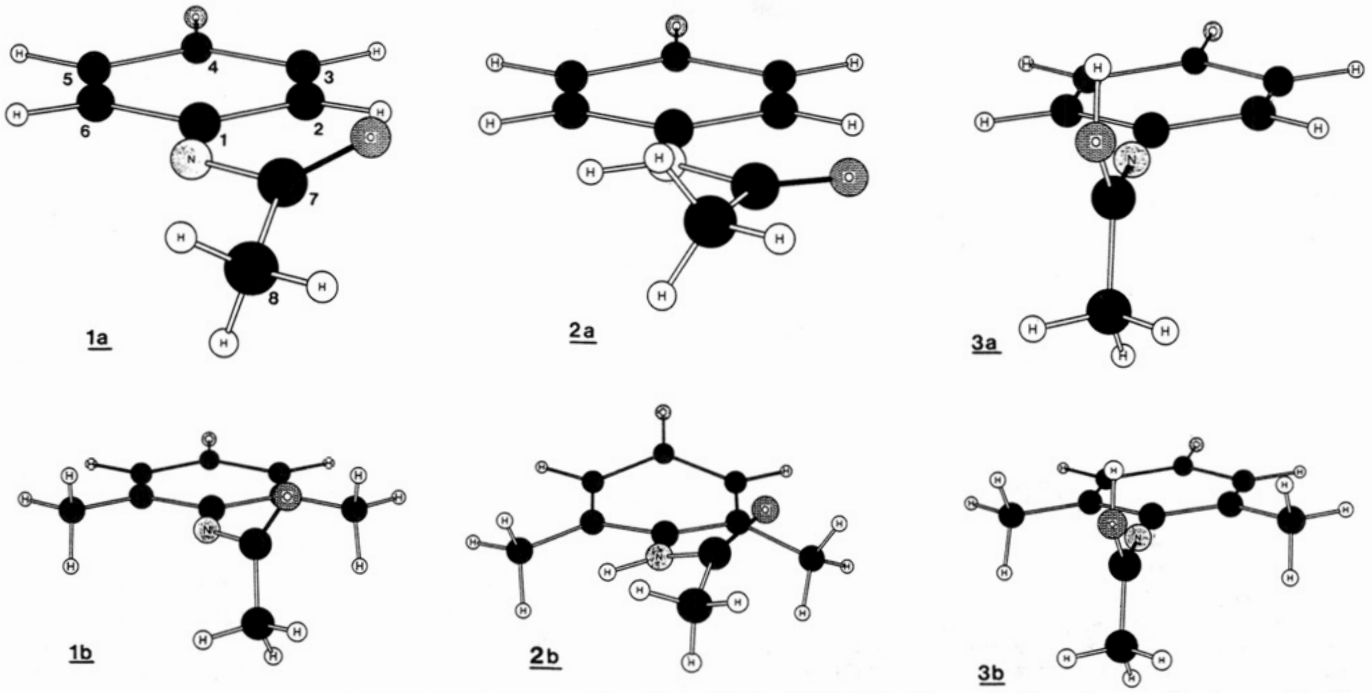

Figure 2. Perspective drawings of **1–3a** and **1–3b** taken from the optimized 3-21G structures. Carbon atom numbering used in the text is indicated for **1a**.

(see Experimental Section). It is likely that the oxidation of 4-aminophenol by Ag_2O in CH_3CN does not proceed quantitatively to **4a** and the apparently low yields of *p*-benzoquinone are due to lower than calculated stock solution concentrations.

Plots of log k_0 vs pH for both **4a** and **4b** (Figure 1) show the titration of an ionizable proton. The data in Figure 1 were fit to eq 5 by nonlinear least-squares methods to

$$k_0 = \left(\frac{[H^+]}{K_a^N + [H^+]}\right)k_s \qquad (5)$$

obtain the kinetic parameters in Table II. The pK_a^N of **5a** has been measured previously by both kinetic[16] and equilibrium methods[17] to be 3.7 and 3.9 under conditions very similar to our own. The initial absorbance of solutions of **4b** at 275 nm in the hydrolysis reaction mixtures also varies with pH in a manner consistent with titration of an ionizable proton. The pK_a^N estimated from the data (Figure 1) is 3.00 ± 0.04.

The ΔpK_a^N (**5a** − **5b**) of 0.7 does indicate that the methyl groups of **5b** affect pK_a^N by other than electronic means. The measured ΔpK_a for the conjugate acids of pyridine and 3,5-dimethylpyridine is −1.0.[18] The methyl substituents of 3,5-dimethylpyridinium ion have bond connectivity with respect to the nitrogen atom identical with that in **5b**, but are situated in space so that, presumably, their only effect on pK_a is electronic in nature.

Restricted Hartree–Fock calculations were performed on structures **1–5a** and **1–5b** with the GAUSSIAN86 and GAUSSIAN88 programs.[9] Complete geometry optimizations were performed on all ten structures at the STO-3G[10] and 3-21G[11] levels. Single-point calculations at the 6-31G* level with second-order Moller–Plesset correlation energy corrections were performed in selected cases on the optimized 3-21G structures.[14,15] The total energies determined for these species at the various levels are presented in Table III. The optimized STO-3G and 3-21G structures are presented in Table IV in the supplementary material. In Figure 2 perspective drawings for **1–3a** and **1–3b** at the 3-21G level are shown. With the exception of **2b** all structures contain an essentially planar quinone imine ring system at both the STO-3G and 3-21G levels. In **1a** the twist angle of the amide carbonyl, with reference to the N=C_1 bond is 27.9° in the 3-21G structure (Figure 2) and 52.7° in the STO-3G structure. Figure 3 shows that rotation about the C_7(O)–N bond from 0° to approximately 90° occurs relatively freely according to the STO-3G calculations with only a 1.5 kcal difference between the highest and lowest energy conformer in this range. The rotational barriers calculated and observed for ordinary amides are much larger, on the order of 15–20 kcal/mol.[19,20]

Table III. Total Energies of 1–5a and 1–5b Calculated by ab Initio Methods

	energy (hartrees)[a]		
species	STO-3G	3-21G	6-31G*//3-21G
1a	−504.644 078	−508.293 437	−511.167 250 (−512.670 459)[b]
1b	−581.807 507	−585.937 656	−589.241 005 (−591.016 507)[b]
2a	−505.095 433	−508.664 615	−511.527 383 (−513.022 671)[b]
2b	−582.255 126	−586.297 611	−589.593 543 (−591.362 709)[b]
3a	−505.071 290	−508.647 584	
3b	−582.245 552	−586.299 256	
4a	−354.822 371	−357.368 415	−359.393 364
4b	−431.992 706	−435.018 439	−437.472 518
5a	−355.272 124	−357.745 849	−359.759 833
5b	−432.445 571	−435.397 672	−437.842 113

[a] The STO-3G and 3-21G results are from completely optimized structures. The 6-31G* results are single point calculations on the optimized 3-21G structures. [b] This energy includes the second-order Moller–Plesset correlation correction.

(16) Corbett, J. F. *J. Chem. Soc. B* **1969**, 213–216.
(17) Fieser, L. F. *J. Am. Chem. Soc.* **1930**, *52*, 4915–4940.
(18) Clarke, K.; Rothwell, K. *J. Chem. Soc.* **1960**, 1885–1895.
(19) (a) Zielinski, T. J.; Poirier, R. A.; Peterson, M. R.; Csizmadia, I. G. *J. Comp. Chem.* **1982**, *3*, 477–485. (b) Shipmann, L. L.; Christofferson, R. E. *J. Am. Chem. Soc.* **1973**, *95*, 1408–1416. (c) Nalewajski, R. F. *J. Am. Chem. Soc.* **1978**, *100*, 41–46.

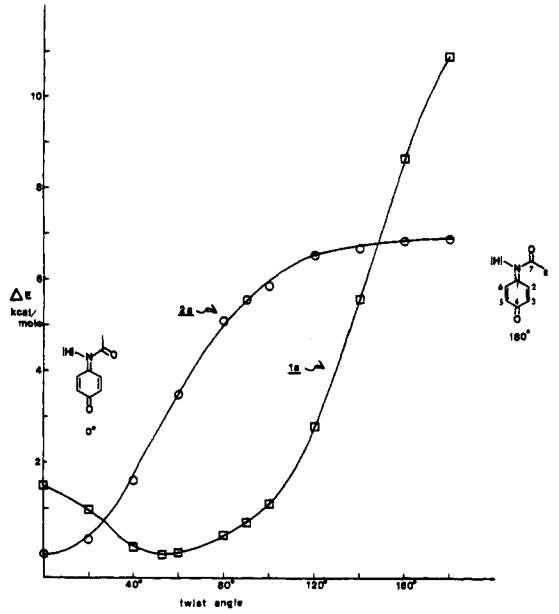

Figure 3. Relative energy as a function of the C_7=O, N=C_1 twist angle for **1a** and **2a**. Energies were calculated at the STO-3G level. Geometries were completely optimized at each fixed rotation angle.

In **1a** the low rotational barrier occurs because the π^* orbital of the amide carbonyl can interact with both the nonbonding orbital on N and the π orbital of the N=C_1 bond. The optimal geometries for these interactions occur at 90° and 0° twist angles, respectively. STO-3G calculations performed at twist angles of 0°, 52.7°, and 90° show that the C_7–N bond length changes very little with rotation from 1.4779 to 1.4758 to 1.4785 Å, respectively. The C–N bond length for formamide changes from 1.4026 Å (at the planar minimum) to 1.4806 Å (for the transition state for rotation about the C–N bond) at the STO-3G level. The calculated energy barrier is 6.0 kcal/mol in formamide. Calculations at the 3-21G level show a bond length change from 1.3533 to 1.4310 Å and an energy barrier of 18.6 kcal/mol for formamide.[19a] At twist angles above 90° the energy rapidly increases due to nonbonding interactions between the acyl methyl group and the quinone imine ring. In the 180° conformer, the center-to-center distances between the hydrogen on C_2 (Figure 3) of the quinone imine ring and two of the hydrogens of the acyl methyl group are only 2.13 Å. This is well within the sum of the van der Waal's radii for two hydrogens of 2.4 Å.[21] Bond angle distortions are also noted in the 180° conformer. The C_1–N–C_7 angle of 127.6° and the N–C_7–C_8 angle of 125.2° are significantly larger than the equivalent angles in the lowest energy conformer (118.9° and 112.6°) or the 0° conformer (121.2° and 110.6°). In **1b** the twist angle for the amide carbonyl increases to 75.8° at the STO-3G level and 71.8° at the 3-21G level although the quinone imine ring system remains essentially planar. According to the data in Figure 3, this is well within the range of fairly unrestricted rotation for **1a**. The increase in the twist angle for **1b** is apparently caused by nonbonding interactions involving the acyl oxygen and the ring methyl groups.

Upon protonation of **1a** to generate **2a**, the optimal twist angle for the amide carbonyl reduces to 0.0° at both the STO-3G and 3-21G levels so that the molecule becomes

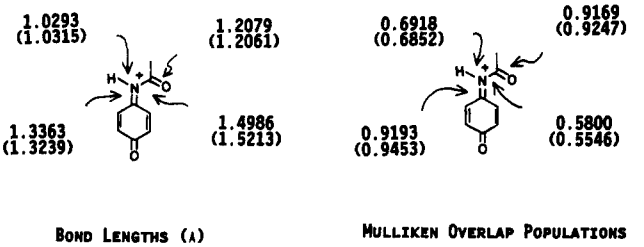

Figure 4. Bond lengths and reduced Mulliken overlap populations calculated at the STO-3G level for the 0° and 90° conformers of **2a**. Data in parentheses are for the 90° conformer.

essentially planar. The data in Figure 3 show that there is a steep rise in energy when the amide carbonyl group is rotated out of this plane. The 90° conformer is 5.6 kcal less stable than the 0° planar conformer at the STO-3G level. The 180° conformer is destabilized largely by nonbonding interactions of the acyl methyl group with the quinone imine ring as previously indicated for **1a**.

Bond length and reduced Mulliken overlap population differences between the 0° and 90° conformers of **2a** are summarized in Figure 4. These changes indicate significant interaction between the carbonyl and imine π systems in the 0° conformer. In the 90° conformer no such interaction is possible and the relatively high energy nonbonding orbital on N is no longer available for interaction with the π^* orbital of the carbonyl group.

Calculations on the N-protonated conjugate acids of ordinary amides indicate essentially free rotation for these species about the C(O)–N bond with rotational barriers of 1.0 kcal/mol or less.[19] In these compounds N-protonation removes the possibility of delocalization of the nitrogen lone pair so that little or no barrier to rotation remains after protonation. In **2a** π-delocalization does occur in the planar conformers, which leads to a significant barrier to rotation.

The 2,6 dimethyl groups of **2b** prevent this species from taking on a conformation similar to the lowest energy conformer of **2a**. At both the STO-3G and 3-21G levels the quinone imine ring of **2b** is significantly distorted out of planarity (Figure 2). Since the ring in **2a** remains essentially planar throughout the bond rotation shown in Figure 3, the distortion of the ring in **2b** cannot be due simply to rotation about this bond. A partial optimization of **2b**, which restricted the ring to a plane, was performed at the STO-3G level. This calculation showed that the planar conformer was 0.5 kcal higher in energy than the nonplanar conformer calculated with complete geometry optimization. Given the limitations of the STO-3G basis set and the Hartree–Fock method, it is impossible to tell what the true minimum energy conformation of **2b** is. The reasons for the low energy nonplanar conformer are apparent though. In the planar conformer of **2b** the amide carbon is twisted 13.7° out of the ring plane and the twist angle of the carbonyl group with respect to N=C_1 is 45.6°. In the STO-3G structure of **2a** both of these angles are 0.0°. Even with these distortions the carbonyl oxygen is within 2.24 Å of the nearest hydrogen on the ring methyl group. The calculations suggest that **2b** distorts into nonplanarity to avoid some of the severe nonbonding interactions present in the planar conformer.

The calculated structures of **3a** and **3b** are very similar with an essentially linear arrangement of C_1, N, and C_7 (Figure 2) and short C_1–N and C_7–N bonds (1.2606 and 1.2520 Å, respectively, at the 3-21G level for **3a**). The conformers in which the dihedral angle for rotation of the O–H bond about the C_7–N bond is 0° are the most stable according to our calculations.

(20) Sunners, B.; Piette, L. H.; Schneider, W. G. *Can. J. Chem.* **1960**, *38*, 681–688. Kamei, H. *Bull, Chem. Soc. Jpn.* **1968**, *41*, 2269–2273. Drakenberg, T.; Forsen, S. *J. Phys. Chem.* **1970**, *74*, 1–7. Ross, B. D.; True, N. S. *J. Am. Chem. Soc.* **1984**, *106*, 2451–2452.

(21) Murrell, J. N.; Kettle, S. F. A.; Tedder, J. M. *The Chemical Bond*, 2nd ed.; Wiley: New York, 1985; p 42.

Table V. Calculated ΔE for the Reactions of Equations 6–8

	ΔE (kcal/mol)		
reaction	STO-3G	3-21G	6-31G*//3-21G
6	−1.95	−1.13	−1.96
7	2.34	7.06	4.77 (3.77)[a]
8	−6.80	−4.68	

[a] Includes second-order Moller–Plesset correlation energy correction.

Discussion

The data in Table III can be used to estimate energy changes associated with gas-phase proton transfer involving the species **1–5**. The ΔE for the equilibria represented by eqs 6–8 are presented in Table V. These equilibria were

$$\mathbf{5a} + \mathbf{4b} \rightleftharpoons \mathbf{4a} + \mathbf{5b} \quad (6)$$

$$\mathbf{2a} + \mathbf{1b} \rightleftharpoons \mathbf{1a} + \mathbf{2b} \quad (7)$$

$$\mathbf{3a} + \mathbf{1b} \rightleftharpoons \mathbf{1a} + \mathbf{3b} \quad (8)$$

chosen to minimize ΔS so that, to a first approximation, ΔE can be taken as a measure of ΔG for these reactions.

These data show that proton transfer from **5a** to **4b** (eq 6) is thermodynamically favorable in the gas phase. ΔE at the 6-31G*//3-21G level corresponds to an intrinsic contribution to ΔpK_a^N (**5a** − **5b**), $\Delta pK_{a_I}^N$, of −1.5 at 20 °C. If we assume that the measured ΔpK_a^N in H_2O (0.7) is composed of an intrinsic and solvent contribution (eq 9), then the solvent contribution, $\Delta pK_{a_{sol}}^N$, for **5a** and **5b** is 2.2.

$$\Delta pK_a^N = \Delta pK_{a_I}^N + \Delta pK_{a_{sol}}^N \quad (9)$$

Available data on similar systems indicate that these results are reasonable. Since the bond connectivity of the methyl substituents with respect to N is equivalent for **5b** and 3,5-dimethylpyridinium ion, the measured ΔpK_a^N for pyridinium ion and 3,5-dimethylpyridinium ion of −1.0 at 20 °C[18] provides an estimate of $\Delta pK_{a_I}^N$ for **5a** and **5b**. The 6-31G*//3-21G estimate of −1.5 for $\Delta pK_{a_I}^N$ is in reasonable agreement with this. The effect of steric hindrance of solvation on the pK_a^N of 2,6-di-*tert*-butylpyridinium ion (**6**) has been estimated to be −2.2 in 50% EtOH at 25 °C.[3a]

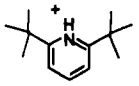

6

The structures of **6** and **5b** are very similar in the vicinity of the acidic proton and the 3-21G calculations indicate that each of the N–H protons of **5b** is only 2.29 Å distant from the two nearer hydrogens of the methyl groups.

Proton transfer from **2a** to **1b** (eq 7) is unfavorable in the gas phase at all levels of theory examined. The 6-31G*//3-21G results indicate a $\Delta pK_{a_I}^N$ (**2a** − **2b**) of 3.6 without the correlation energy correction and 2.8 with it. The major differences in the gas-phase proton-transfer equilibria involving the acylated and deacylated imines can be attributed to the instability of **2b**, which is caused by the steric interactions described above.

Unlike **5b**, **2b** may not have a planar structure but the acidic proton is still within 2.2 Å of the two nearest hydrogens on the methyl group bonded to C-6 (Figure 2) in both the planar and nonplanar structures of **2b** at the STO-3G level. Solvent access to this proton must be limited. If the value of 2.2 estimated for $\Delta pK_{a_{sol}}^N$ for **5a** and **5b** is used in the present case, the ΔpK_a^N for **2a** and **2b** is approximately 5.0 to 5.8. This is only in moderate agreement with the value of 3.2 estimated from kinetic data,[2] but considering the number of approximations made in arriving at both values the agreement is satisfactory. The results presented here do indicate that two factors play a role in determining ΔpK_a^N for **2a** and **2b**: steric hindrance to solvation of the acidic proton and sterically enforced conformational differences in the structures of **2a** and **2b** which lead to destabilization of **2b**.

The effects of the methyl substituents on O-protonation of **1a** and **1b** is considerably different than their effect on N-protonation. Results in Table V show that proton transfer from **3a** to the acyl oxygen of **1b** is thermodynamically favorable at both the STO-3G and 3-21G levels. This is due to a combination of the electronic effect of the methyl substituents and release of some steric strain upon O-protonation of **1b**. The linear arrangement of C_1, N, and C_7 reduces nonbonding interactions between the ring methyls and the acyl group to a minimum.

The calculations indicate that **2a** is more stable than **3a** by 10.7 kcal/mol at the 3-21G level while **2b** and **3b** are of very similar stability with **3b** favored by 1.0 kcal/mol. Both calculations and experimental data indicate that O-protonation is greatly favored over N-protonation for ordinary amides.[19a,22,23] This is due in large part to the loss of delocalization involving the nitrogen lone pair upon N-protonation. The rotation angle calculations of Figure 3 for **1a** and **2a** indicate that this factor is mitigated for **1a** because of the availability of π-delocalization in the planar conformer. This delocalization is maintained in the N-protonated conjugate acid.

The ab initio calculations provide evidence against the O-protonation mechanism of eq 2 for the specific acid catalyzed hydration of **1**. If the reaction proceeded via the O-protonation mechanism, the hydration rate constant for **1b** should be larger than that for **1a** due to the apparent greater ease of O-protonation of **1b** and the lack of any substantial effect of the 2,6-dimethyl group on the attack of small nucleophiles on C-1.[2] In fact, the specific acid catalyzed hydration rate constant for **1a** is 7.7×10^3 fold larger than that for **1b**.[2] Our results indicate that the N-protonation mechanism of eq 1 would be slower for **1b**, in accord with observation.

These results and our previous data on the hydrolysis reaction of **1a** and **1b**[2] show that the chemistry of *N*-acyl imines and ordinary amides are quite different. Our calculations indicate that N-protonation is thermodynamically favored in *N*-acyl imines if steric factors do not play a significant role, while it is very clear that O-protonation is thermodynamically favored for ordinary amides.[19a,22,23] The availability of π-delocalization in the planar conformers of *N*-acyl imines lowers the rotational potential of the C(O)–N bond in the unprotonated species and makes a planar conformer the lowest energy conformation of the N-protonated species. This is also an important factor in stabilizing the N-protonted form vs its O-protonated isomer. Acid-catalyzed hydrolysis of *N*-acyl imines appears to occur via attack of H_2O on the imine carbon of the N-protonated conjugate acid under dilute acid conditions. We found no evidence for competing hydrolysis of the C(O)–N bond in either **1a** or **1b**,[2] and an earlier study of the hydrolysis of benzophenone *N*-acyl imines also found only hydrolysis of the imine bond under dilute acid conditions.[24] Amide hydrolysis via the O-

(22) Bonaccorsi, R.; Pullman, A.; Scrocco, E.; Tomasi, J. *Chem. Phys. Lett.* **1972**, *12*, 622–624. Pullman, A. *Chem. Phys. Lett.* **1973**, *20*, 29–32. Hopkinson, A. C.; Csizmadia, I. G. *Can. J. Chem.* **1973**, *51*, 1432–1434.

(23) Fersht, A. R. *J. Am. Chem. Soc.* **1971**, *93*, 3504–3515. Martin, R. B. *J. Chem. Soc., Chem. Commun.* **1972**, 793–794. Kresge, A.; Fitzgerald, P. H.; Chiang, Y. *J. Am. Chem. Soc.* **1974**, *96*, 4698–4699.

(24) Sayer, J. M.; Conlan, P. *J. Am. Chem. Soc.* **1980**, *102*, 3592–3600.

protonation mechanism[25] is not observed because of the relative difficulty of O-protonation in *N*-acyl imines and the availability of a low energy path for imine hydrolysis in these compounds.[2,24]

Acknowledgment. This work was supported, in part, by a grant from the National Institutes of General Medical Sciences (GM 38449-01). A grant of computer time on the Cray Y-MP8/864 at the Ohio Supercomputer Center is also gratefully acknowledged (POS075-1), as is the help of the Miami University Academic Computer Service in installing and testing GAUSSIAN86 at Miami. We would also like to thank Professor Gilbert Gordon of this department for the use of his rapid scan stopped flow spectrophotometer and Dr. Istvan Fabian for his technical assistance with this instrument.

Supplementary Material Available: Table I listing hydrolysis rate constants for **1a** and **1b** and Table IV listing optimized STO-3G and 3-21G structures for **1-5a** and **1-5b** (14 pages). Ordering information is given on any current masthead page.

(25) Kresge, A. J.; Fitzgerald, P. H.; Chiang, Y. *J. Am. Chem. Soc.* **1974**, *96*, 4698-4699. Williams, A. *J. Am. Chem. Soc.* **1976**, *98*, 5645-5651.

Experimental and Theoretical Study of Orientation in the Nitration of Dithieno[3,4-*b*:3′,4′-*d*]pyridine

Kalman J. Szabo, Anna-Britta Hörnfeldt, and Salo Gronowitz*

Division of Organic Chemistry 1, Chemical Center, University of Lund, P.O. Box 124, S-221 00 Lund, Sweden

Received June 11, 1990

The nitration of dithieno[3,4-*b*:3′,4′-*d*]pyridine was investigated. Despite the similarity of the electrophilic reaction centers, high positional selectivity was found. Thus, the 1-, 8-, and 3-nitro isomers were obtained in the relative amounts 78%, 20%, and 2%, respectively. In spite of the unusually large size of the molecular systems, the structure and electronic properties of the Wheland intermediates (sigma complexes) and the transition states were calculated at the ab initio 3-21G* level. Harmonic frequencies have been calculated to characterize the stationary points obtained. The Wheland intermediate model failed to predict the site preferences, probably due to steric hindrance. However, the energies found for the transition-state complexes are in good agreement with the experimental findings. The transition-state geometry of the ring system shows greater similarity to the parent structure than to the Wheland intermediate. Orientation effects could be explained by the electron distribution of the transition-state structures.

One of the greatest successes of theoretical organic chemistry is the explanation of the orientating effects of substituents in benzene derivatives in electrophilic substitution reactions.[1] However, although these qualitative rules give reliable results in predicting the isomer distribution in the nitration of aromatic hydrocarbons, they often fail to interpret the results found in the substitution of heterocyclic compounds. This is a consequence of the quite complicated electronic and steric effects, particularly in systems containing several rings and heteroatoms.

There is a considerable current interest in effects that arise from the fusion of several nonequivalent monocycles. Klemm[2] pointed out that the thienopyridine systems should be particularly pertinent for a study of the effects of ring interactions of the monocyclic components (thiophene and pyridine).

We investigated the nitration reaction of dithieno[3,4-*b*:3′,4′-*d*]pyridine (1). This ring system is especially interesting as it contains four nonequivalent thiophenic α-positions. The C_{2v} symmetry of the benzo analogue is decreased only by the nitrogen atom. These two facts suggest a similar reactivity for all the electrophilic centers. In contrast, the experimental results showed high positional selectivity.

The present combined experimental and theoretical investigation was undertaken to gain more insight into the nature of the directing and activating effects in this dithienopyridine ring system.

Experimental Results

The parent compound 1 was nitrated in strong acidic medium (TFA) with nitric acid. Modie et al. demonstrated that the nitration of quinoline and isoquinoline takes place through the conjugate acid under similar conditions.[3] Since the pK_a value for the thienopyridines and isoquinoline are of the same magnitude,[4] it is highly probable that the same is true for the dithieno analogue 1. This is supported by the fact that the nitrate salt of 1 can be precipitated by adding nitric acid to its ethereal solution. Under these conditions, nitration of thiophene rings take place partly via nitrosation followed by oxidation.[5] In order to avoid this side reaction, on determination of isomer distribution, urea was added to remove the nitrous acid.[5] Without this precaution the amount of the 8-nitro derivative is somewhat higher in the reaction mixture (60% 1-nitro, 38% 8-nitro, and 2% 3-nitro derivative). The results of the competitive nitration (eq 1) show that position 1 (2) is the most reactive followed by position 8 (4) and position 3 (3). We could not detect any nitration in position 6 nor in position 5. The nitro isomers are all crystalline products with high melting points. Their sol-

(1) Ingold, C. K. *Structure and Mechanism in Organic Chemistry*; Cornell University Press: London, 1969; pp 264-418.
(2) Klemm, L. H. *Heterocycles* **1981**, *15*, 1285-1308.
(3) Modie, R. B.; Schöfield, K.; Wiliamson, M. J. *Chem. Industry* **1963**, 1283-1284.
(4) Gronowitz, S.; Sandberg, E. *Arkiv Kemi* **1970**, *32*, 217-227.
(5) Butler, A. R.; Hendry, J. B. *J. Chem. Soc. B* **1971**, 102-105.

0022-3263/91/1956-1590$02.50/0